Hindawi
Advances in Materials Science and Engineering
Volume 2019, Article ID 2735328, 10 pages
https://doi.org/10.1155/2019/2735328

Research Article

Effects of Adhesive Parameters on Dispersion Characteristics of Ultrasonic Guided Waves in Composite Pipes

Juanjuan Li [1,2] and Yan Han [1]

[1] *Shanxi Key Laboratory of Signal Capturing & Processing, North University of China, Taiyuan 030051, China*
[2] *Lvliang University, Lvliang 033000, China*

Correspondence should be addressed to Juanjuan Li; jujunuc@gmail.com

Received 5 September 2019; Accepted 23 October 2019; Published 16 December 2019

Academic Editor: Md Mainul Islam

The aim of the investigation presented here was to understand how the viscosity parameters of an adhesive layer affect group velocity and attenuation of the double-layer adhered pipe. Various parameter combinations (attenuation of longitudinal wave and shear wave, $p\alpha_L$ and $q\alpha_T$; thickness, d; and density, $n\rho$) were utilized in order to generate different uncured degrees of the adhesive layer. In the frequency range 0~500 kHz, the group velocity dispersion curves and attenuation dispersion curves were obtained from these models. Then, the group velocity and attenuation of the two commonly used modes, $L(0,2)$ and $T(0,1)$, were compared and analyzed. The results have shown that it is important to remark that little effect on group velocity was caused, and significant linear increases of attenuation occur with increase in q, d, and n. However, variable p had little effect on attenuation; more modes emerged when d increased or n decreased, causing difficulties on mode identification and signal processing. The numerical results provided a useful way to evaluate bonding quality by measuring the group velocity and attenuation in the pipelines.

1. Introduction

Glass fiber reinforced pipes (GFRP) are widely applied to aerospace, construction, chemical equipment, medical devices, sports equipment, and other fields because of many advantages, such as high-pressure resistance, corrosion preventive, excellent flexibility, convenient installation, long service life, and so on. The adhesive layer can transmit stress, block crack, and absorb and scatter energy. A poorly cured interface can degrade the viscoelastic strength, which may cause fatigue cracks, and a debonding interface can reduce the mechanical properties, which may cause brittle failure. The existence of uncured defects will inevitably affect the safety and reliability of pipelines in use. Therefore, it is of great significance to carry out bonding quality inspection of composite pipes online and in service.

Conventional ultrasonic nondestructive testing (NDT) methods become difficult and inefficient to evaluate bonding quality of pipelines [1–7]. Guided wave is widely used in nondestructive inspection because of its capacity of traveling long distances without substantial attenuation [8–12]. However, guided wave signals are difficult to analyze due to the multimode and dispersion characteristics. Based on material properties of the adhesive layer, the dispersion behavior can be described by obtaining the group velocity curve and attenuation curve with the different adhesive quality [13–15].

To date, several studies have been investigated by many scholars to inspect bonded structures and have proved that guided wave detection is a very effective method. Matt [16] performed semianalytical finite element (SAFE) analyses for CFRP plate-to-spar joints in unmanned aerial vehicles and provided substantial insight into the guided wave behavior within pristine and damaged joints; the SAFE method was adopted to the dispersive properties of the guided wave across a pipe elbow and in materials with viscoelastic properties (Shorter [17]; Lhémery et al. [18]; Yan et al. [19]); Scalea et al. [20] studied the propagation of guided waves in adhesively bonded lap shear joints. The lowest-order, antisymmetric A_0 strength of transmission was studied for three different bond states in aluminum joints. Hong [21] combined Hamilton's principle and the semianalytical finite element method to study phase velocity dispersion curves of 16 layer adhesively bonded composites. The result showed phase velocity changed slightly when the state of the adhesive layer changed from properly bond to poorly bond. Siryabe et al. [22] excited the Lamb wave by an air-coupled transducer in the aluminum substrate and analyzed the time-frequency relationship of S_0 under different bonding conditions. Castaings [23] found that SH0 was sensitive to the change of properties of the interfacial adhesive, which can analyze the bonding quality by quantifying the shear properties at the interface. Kharrat et al. [24] selected the torsional wave $T(0,1)$ to detect the defects of pipeline. Rojas et al. [25] combined dispersion curve with short-time wavelet entropy of Lamb mode to detect flat bottom hole defects in the center of the plates.

In summary, most of the literature on guided waves focused on the propagation of elastic materials with little or no damping, not considering the effect of material absorption on guided wave attenuation, and research objects are more focused on the plate structure and lap joints. Therefore, the dispersion characteristics of the bonded composite pipes are studied in this paper. Based on the fact that the defects of bonding structures are mainly related to acoustic properties, thickness, and density of the adhesive layer, this paper mainly studied the effect of these variations on dispersion characteristics of guided waves.

2. Basic Theory of Guided Wave in Pipes

In a cylindrical structure with a global cylindrical coordinate system (r, θ, z), as shown in Figure 1, guided waves can propagate in the axial or circumferential direction. SAFE has been widely adopted for the computation of guided wave dispersive features in waveguides. Navier's governing guided wave equation can be expressed as the following equation [8, 26]:

$$\int_V \delta u^T \cdot \rho \ddot{u}\, \mathrm{d}V + \int_V \delta \varepsilon^T \cdot \sigma\, \mathrm{d}V = 0, \tag{1}$$

where $\int_V \mathrm{d}V$ are the volume integral, $\mathrm{d}V = r\mathrm{d}r\mathrm{d}\theta\mathrm{d}z$; $\ddot{u}$ is the second derivative of displacement u with respect to time t, $\ddot{u} = \partial u^2/\partial t^2$; T represents the matrix transpose; r is the density; ε is the strain; and σ is the stress.

Assuming that guided waves propagate in the z direction, the displacement $u(r,\theta,z,t)$ can be represented by the following equation:

$$u(r,\theta,z,t) = \sum_{j=1}^{2} N(r) U^j e^{i(kz+n\theta-\omega t)}, \tag{2}$$

where U^j is the nodal displacement vector of the j_{th} element and $N(r)$ is the shape function with respect to the thickness r. For a two-node element, $N(r)$ is a 3×6 matrix, as follows: where

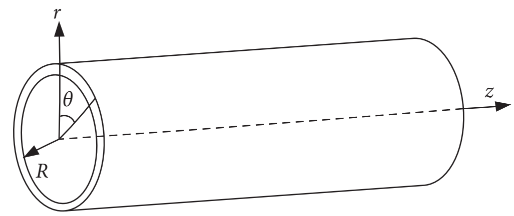

Figure 1: Hollow cylinder axes configuration.

$$N = \begin{bmatrix} N_1 & 0 & 0 & N_2 & 0 & 0 \\ 0 & N_1 & 0 & 0 & N_2 & 0 \\ 0 & 0 & N_1 & 0 & 0 & N_2 \end{bmatrix},$$
$$N_1 = \frac{1}{2}(1-\xi),$$
$$N_2 = \frac{1}{2}(1-\xi). \tag{3}$$

$-1 \le \xi \le 1$ is the natural coordinate in the r direction. The strain-displacement relations in cylindrical coordinates is as follows:

$$\varepsilon = [\varepsilon_{rr}, \varepsilon_{\theta\theta}, \varepsilon_{zz}, \gamma_{\theta z}, \gamma_{rz}, \gamma_{r\theta}], \tag{4}$$

in which

$$\begin{aligned} \varepsilon_{rr} &= \frac{\partial u_r}{\partial r}, \\ \varepsilon_{\theta\theta} &= \frac{u_r}{r} + \frac{1}{r}\frac{\partial u\theta}{\partial \theta}, \\ \varepsilon_{zz} &= \frac{\partial u_z}{\partial z}, \\ \gamma_{\theta z} &= \frac{1}{r}\frac{\partial u_z}{\partial \theta} + \frac{\partial u_\theta}{\partial z}, \\ \gamma_{rz} &= \frac{1}{r}\frac{\partial u_r}{\partial z} + \frac{\partial u_z}{\partial r}, \\ \gamma_{r\theta} &= \frac{1}{r}\frac{\partial u_r}{\partial \theta} + \frac{\partial u_\theta}{\partial r} - \frac{u_\theta}{r}. \end{aligned} \tag{5}$$

According to Hooke's law, the stress-strain relation is

$$\sigma = C\varepsilon, \tag{6}$$

where C is the stiffness matrix, real in elastic materials, or complex in viscoelastic materials. The elastic constants of all the layers in a composite pipe must be expressed in the global cylindrical coordinate system (r,θ,z). For anisotropic composite materials, this can be achieved through the rotation of the stiffness matrix in the rectangular coordinate system (x, y, z) of each lamina. Substituting the displacement equation (2), strain equation (4), and stress equation (6) into the governing equation (1), eigenvalues for wavenumber k can be solved at each frequency ω and the corresponding eigenvector contains the wave structure information.

Group velocities describe the propagating speeds of guided wave packets, which can be calculated from the wavenumber-frequency relation:

$$C_g = \frac{d\omega}{dk}. \tag{7}$$

If the adhesive material exhibits viscous properties, the viscoelastic matrix C depends on Lame constants λ and μ, considering attenuation coefficients α_L and α_T. The density ρ and Lame constants λ and μ can determine the longitudinal wave velocity c_L^* and shear wave velocity c_T^*, as shown in the following equation:

$$\begin{aligned} c_L^* &= \frac{c_L}{(1 - i\alpha_L)/2\pi}, \\ c_T^* &= \frac{c_T}{(1 - i\alpha_T)/2\pi}, \end{aligned} \tag{8}$$

where $c_L^2 = (\lambda + 2\mu)/\rho$, $c_T^2 = \mu/\rho$. Complex longitudinal wave velocity and complex shear wave velocity are used to solve the Lamb wave problem. A complex wavenumber $k(\omega)^* = k_r(\omega) + ik_i(\omega)$ can be calculated, in which the real part describes the Lamb propagation and the imaginary part represents the Lamb attenuation. The Lamb attenuation caused by the viscosity of the medium is determined by the imaginary part of the complex wavenumber at different frequencies, $k_i(\omega)$.

3. Experimental Works

In the experiment, three layer (GFRP-adhesive-GFRP) pipes (thickness: 0.45 mm/0.1 mm/0.45 mm, inner R: 20 mm) were created. The material parameters of GFRP and adhesive are shown in Tables 1 and 2, respectively.

This paper presents a comprehensive study about the effects of adhesive parameters on the dispersion property of guided waves in composite pipes. Group velocity curves and attenuation curves were obtained using a numerical analysis method in MATLAB language. It is suitable for structures with anisotropic materials and arbitrary shapes, considering the effect of acoustic impedance attenuation.

In view of the large attenuation property of composite materials, the frequency exciting guided wave is usually low. Therefore, the frequency range of this paper was determined to be 0~500 kHz. The viscoelastic parameters of the adhesive were utilized in order to generate some different degree of uncured adhesive layers. For the study, group velocity curves and attenuation curves were obtained from these models (shown in Table 3), where symbols p and q represent the attenuation coefficient of the longitudinal wave and the shear wave, d indicates the thickness, and n is the density coefficient.

Figure 2 shows the group velocity curves about the nonattenuation guided waves with complete solidification. The result showed that there are two longitudinal modes $L(0,1)$ and $L(0,2)$, one torsional mode $T(0,1)$, and three flexural modes $F(1,1)$, $F(1,2)$, and $F(1,3)$. From Figure 2, $L(0,2)$ spreads the fastest and the velocity of $L(0,2)$ and $T(0,1)$ has little change with a frequency above 50 kHz. The normalized wave shapes of these modes in the radial direction with frequency 200 kHz are shown in Figure 3. The result showed that axial and radial displacements are dominant for $L(0,n)$, tangential displacement is dominant for $T(0,1)$, and three displacements exist for $F(m,n)$, respectively.

Table 1: Elastic constants in GPa and mass density in Kg/m^3.

Material	C_{11}	C_{12}	C_{13}	C_{22}	C_{23}	C_{33}	C_{44}	C_{55}	C_{56}	ρ
GFRP	20.3	6	6.5	20.3	6.5	16.2	4.3	4.3	7.1	1853

*From Agostini et al. [27].

Table 2: Wave velocity in m/s, attenuation in Np/λ, and density in Kg/m^3.

Material	c_L	c_T	α_L	α_T	ρ
Adhesive	2410	1210	0.149	0.276	1421

*From Matt [16].

Table 3: Pipe models set for the study.

		Case no.	p	q	d (mm)	n
Effect of body wave attenuation coefficients of adhesive layer	Longitudinal, shear wave attenuation	1	0.5	0.5		
		2	1	1	0.1	1
		3	2	2		
		4	4	4		
	Longitudinal wave attenuation	5	0.5	1		
		6	1		0.1	1
		7	2			
		8	4			
	Shear wave attenuation	9		0.5		
		10		1	0.1	1
		11	1	2		
		12		4		
Effect of thickness of adhesive layer		13			0.5	
		14	1	1	1	1
		15			2	
		16			4	
Effect of density of adhesive layer		17				0.1
		18	1	1	0.1	0.2
		19				0.5
		20				1

4. Results and Discussion

Next, the effects of the adhesive parameters on the dispersion characteristics of guided waves were studied, especially, focused on two typical modes $L(0,2)$ and $T(0,1)$. "C_{L200}" represents the group velocity of $L(0,2)$ at 200 kHz, "A_{T500}" means the attenuation of $T(0,1)$ at 500 kHz, etc.

4.1. Effect of Body Wave Attenuation of Adhesive Layer on Dispersion Curve

4.1.1. $p = q = 0.5$, 1, 2, and 4. Figures 4(a) and 4(b) present the group velocity curves of $L(0,2)$ and $T(0,1)$ when $p = q$.

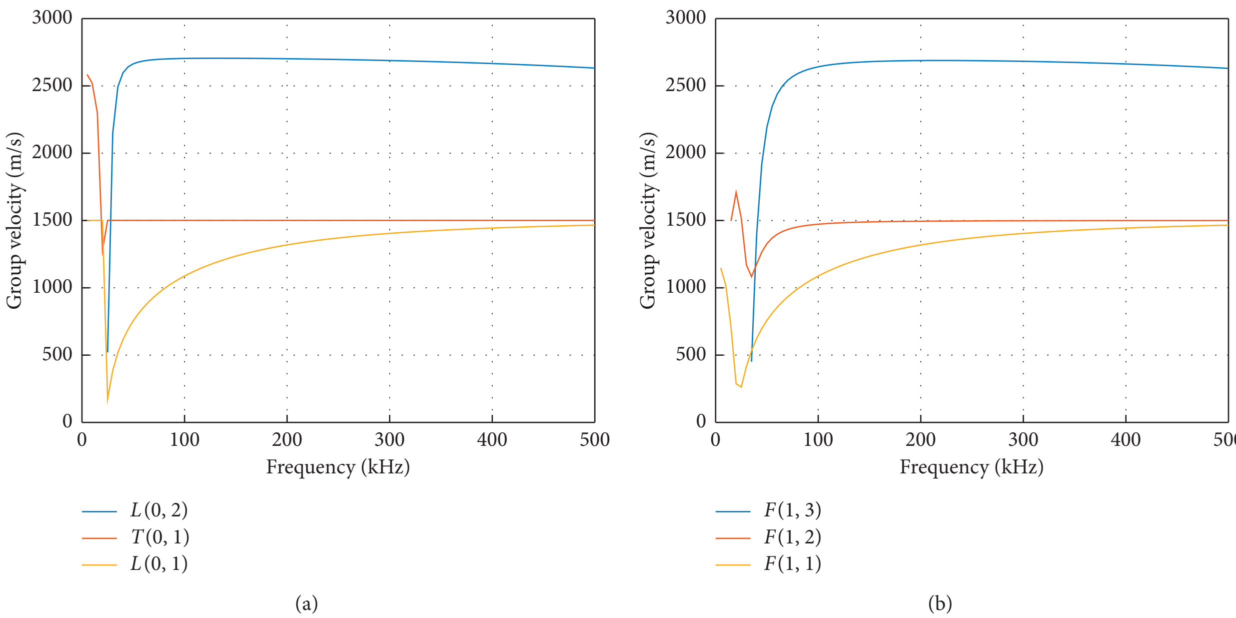

FIGURE 2: Group velocity dispersion curves in pipes with complete solidification, $p = q = 0$. (a) Group velocity curves of the axisymmetric guided wave. (b) Group velocity curves of the nonaxisymmetric guided wave.

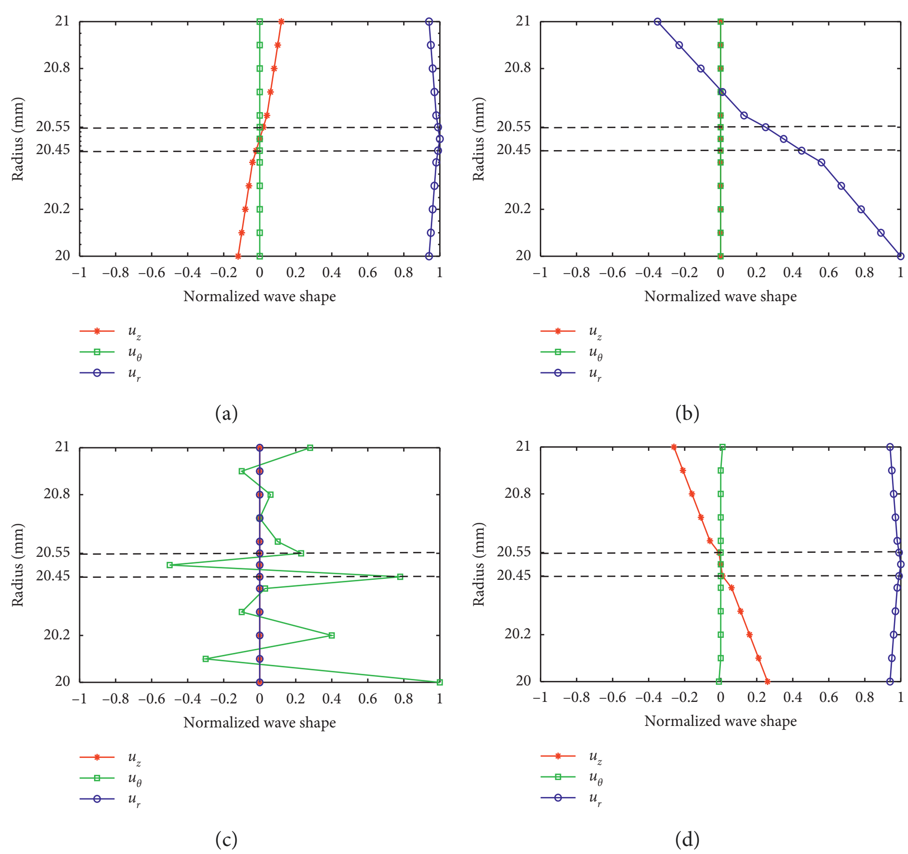

FIGURE 3: Continued.

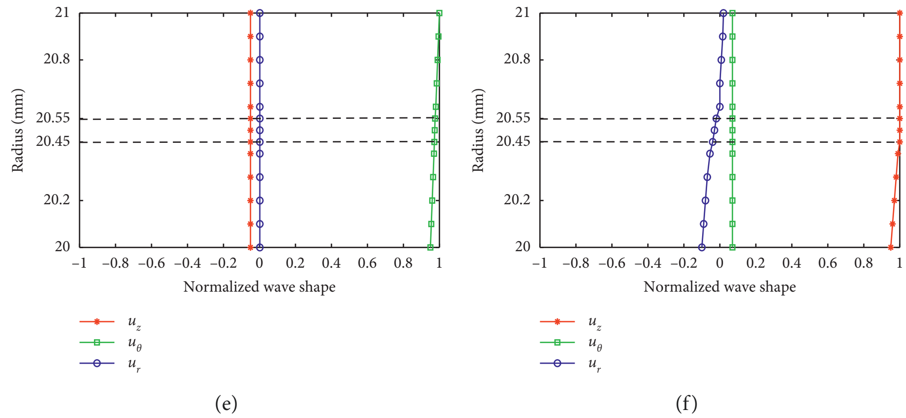

FIGURE 3: Normalized wave shapes of the guided wave at the frequency 200 kHz. (a) $L(0,1)$. (b) $L(0,2)$. (c) $T(0,1)$. (d) $F(1,1)$. (e) $F(1,2)$. (f) $F(1,3)$.

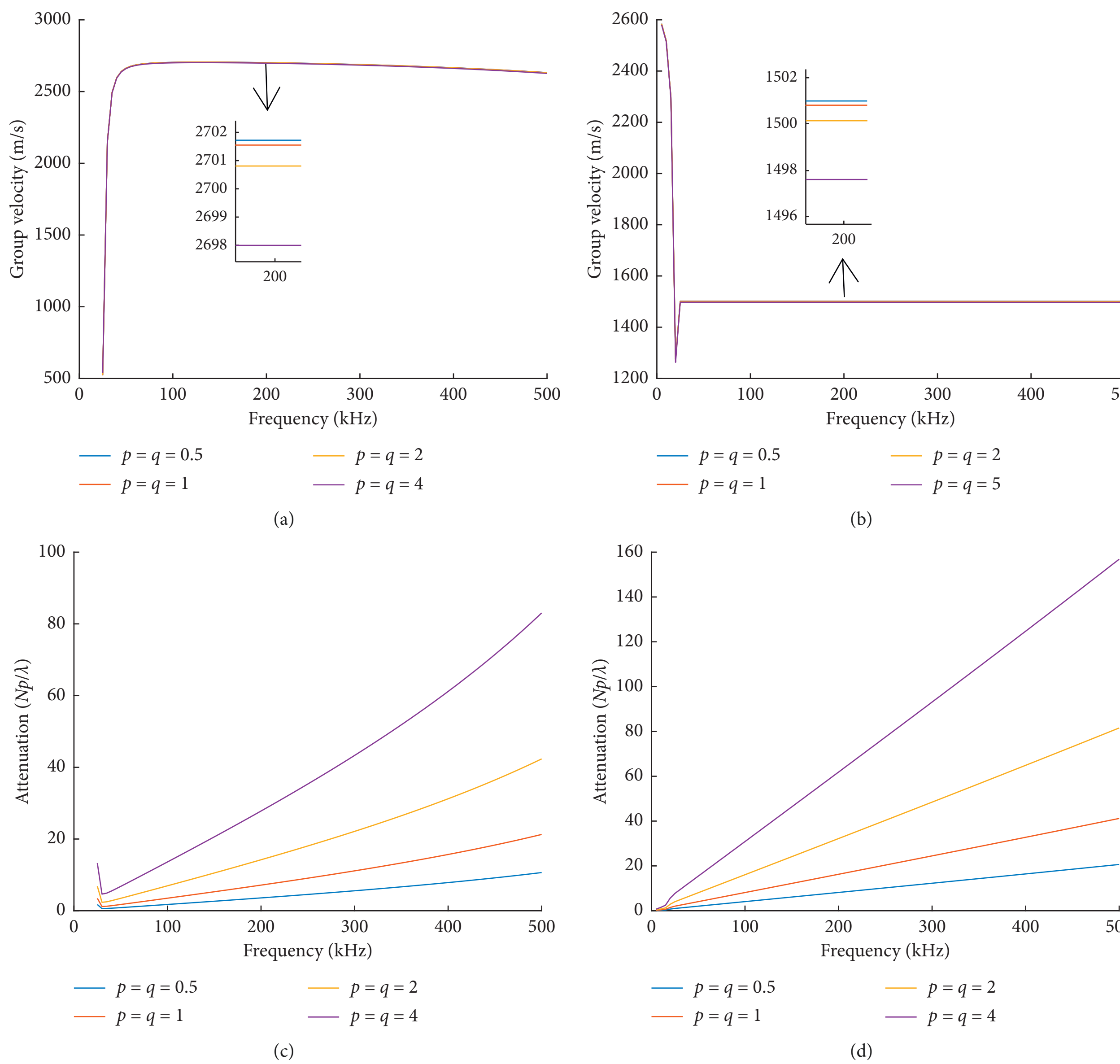

FIGURE 4: Group velocity and attenuation curves of the guided wave, $p = q = 0.5$, 1, 2, and 4. (a) Group velocity curves of $L(0,2)$. (b) Group velocity curves of $T(0,1)$. (c) Attenuation curves of $L(0,2)$. (d) Attenuation curves of $T(0,1)$.

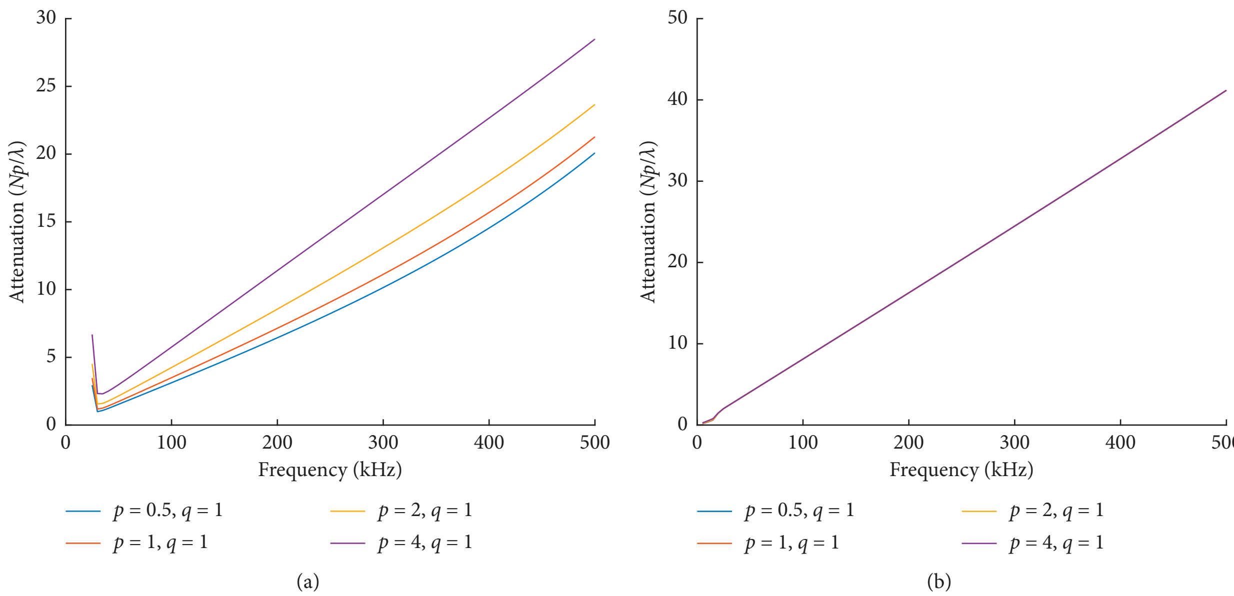

Figure 5: Attenuation curves of guided wave, $p = 0.5$, 1, 2, and 4. (a) Attenuation curves of $L(0, 2)$. (b) Attenuation curves of $T(0, 1)$.

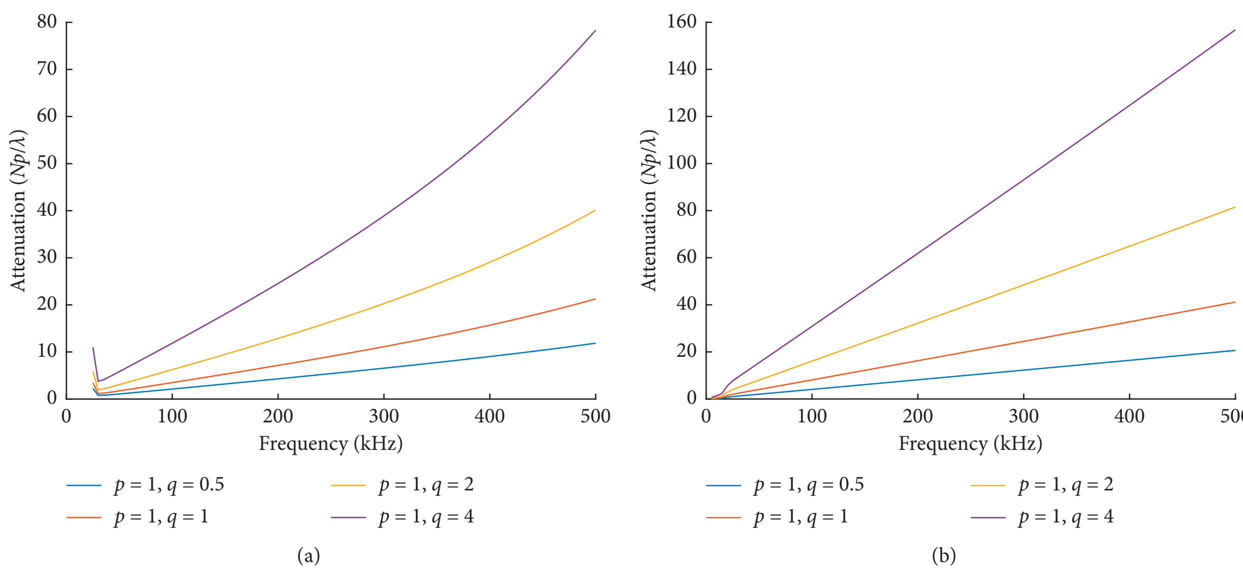

Figure 6: Attenuation dispersion curves of guided wave, $q = 0.5$, 1, 2, and 4. (a) Attenuation curves of $L(0, 2)$. (b) Attenuation curves of $T(0, 1)$.

The curves show that the viscosity of the adhesive layer has little effect (<0.3%) on the group velocity of guided waves. The group velocity range of $L(0, 2)$ is 2698~2702 m/s and of $T(0, 1)$ is 1497~1501 m/s. The attenuation of the viscoelastic material will lead to the imaginary part of the wavenumber. The real part of a complex wavenumber describes the Lamb propagation, and the imaginary part represents the Lamb attenuation. Theoretically, the introduction of body wave attenuation does not affect the group velocity, which is consistent with the experimental results.

Therefore, we will only consider the influence of p, q on the attenuation of guided waves. Figures 4(c) and 4(d) display the attenuation curves of $L(0, 2)$ and $T(0, 1)$ when $p = q$. As shown in Figure 4(c), the attenuation values of $L(0, 2)$ are the lowest at frequency 28 kHz and then gradually increase with the increase in frequency; Figure 4(d) shows that there is generally a linear relationship between the attenuation of $T(0, 1)$ and frequency. In addition, at the same frequency, the greater the value of $p = q$, the higher the attenuation of $L(0, 2)$ and $T(0, 1)$. It is seen that the maximum attenuation value of $L(0, 2)$ is 85 Np/λ and of $T(0, 1)$ is 150 Np/λ, when $p = q = 4$. When $p = q$ is 0.5, 1, 2, and 4, A_{L200}, A_{L500}, A_{T200}, and A_{T500} have 6.77, 679, 659, and 6.60 times growth, respectively (see case 1–case 4).

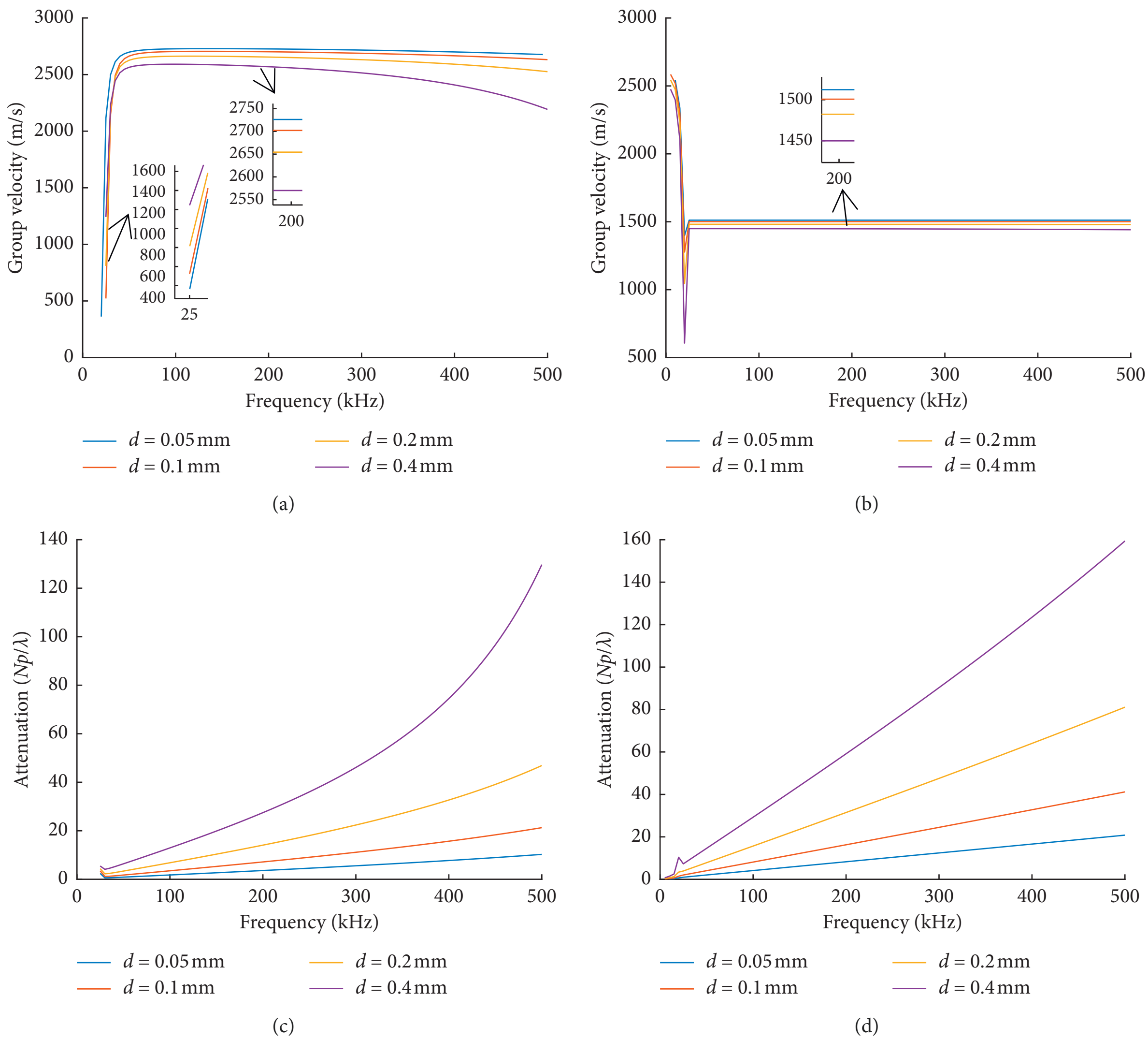

FIGURE 7: Group velocity and attenuation curves of the guided wave, $d = 0.05$ mm, 0.1 mm, 0.2 mm, and 0.4 mm. (a) Group velocity curves of $L(0,2)$. (b) Group velocity curves of $T(0,1)$. (c) Attenuation curves of $L(0,2)$. (d) Attenuation curves of $T(0,1)$.

4.1.2. $p = 0.5$, 1, 2, and 4 and $q = 1$. From Figures 5(a) and 5(b), we can see that while attenuation of $L(0,2)$ gradually increases with the increase in p, the attenuation value of $T(0,1)$ remains unchanged. At frequency 500 kHz, the maximum attenuation values of $L(0,2)$ are 28 Np/λ (see Figure 5(a)) and of $T(0,1)$ are 40 Np/λ (see Figure 5(b)), when $p = 4$ and $q = 1$. When $q = 1$ and p is 0.5, 1, 2, and 4, A_{L200}, A_{L500}, A_{T200}, and A_{T500} have 0.77, 0.36, 0, and 0 times growth, respectively (see case 5–case 8).

4.1.3. $p = 1$ and $q = 0.5$, 1, 2, and 4. The attenuation curves of $L(0,2)$ and $T(0,1)$ are presented in Figures 6(a) and 6(b), illustrating that attenuation of $L(0,2)$ and $T(0,1)$ increases with the increase in q. It is seen that the maximum attenuation value of $L(0,2)$ is about 78 Np/λ and of $T(0,1)$ is about 150 Np/λ, when $p = 1$ and $q = 4$. When $p = 1$ and q is 0.5, 1, and 2, A_{L200}, A_{L500}, A_{T200}, and A_{T500} have 4.57, 5.60, 6.59, and 6.60 times growth, respectively (see case 9–case 12).

The results obtained from the preliminary analysis (see Figures 4–6) are set out to understand that body wave attenuation has little effect on the group velocity dispersion, but causes a significant difference in the attenuation dispersion. What stands out in these figures is that shear wave attenuation has a dominance effect on attenuation dispersion characteristics of guided waves, contrasting the influence of longitudinal wave attenuation. In addition, guided waves in higher frequency will have higher attenuation.

4.2. Effects of Thickness of Adhesive Layer on the Dispersion Curve. The group velocity curves of $L(0,2)$ and $T(0,1)$ with different adhesive thickness are shown in Figures 7(a) and 7(b), respectively. From the curves, it is clear that increasing thickness does result in a slight drop on the group velocity. When d is 0.05, 0.1, 0.2, and 0.4 (mm), C_{L200}, C_{L500}, C_{T200}, and C_{T500} have 5.80%, 18.1%, 4.23%, and 4.70% decrease, respectively. (see case 13–case 16). Figures 7(c) and 7(d) show

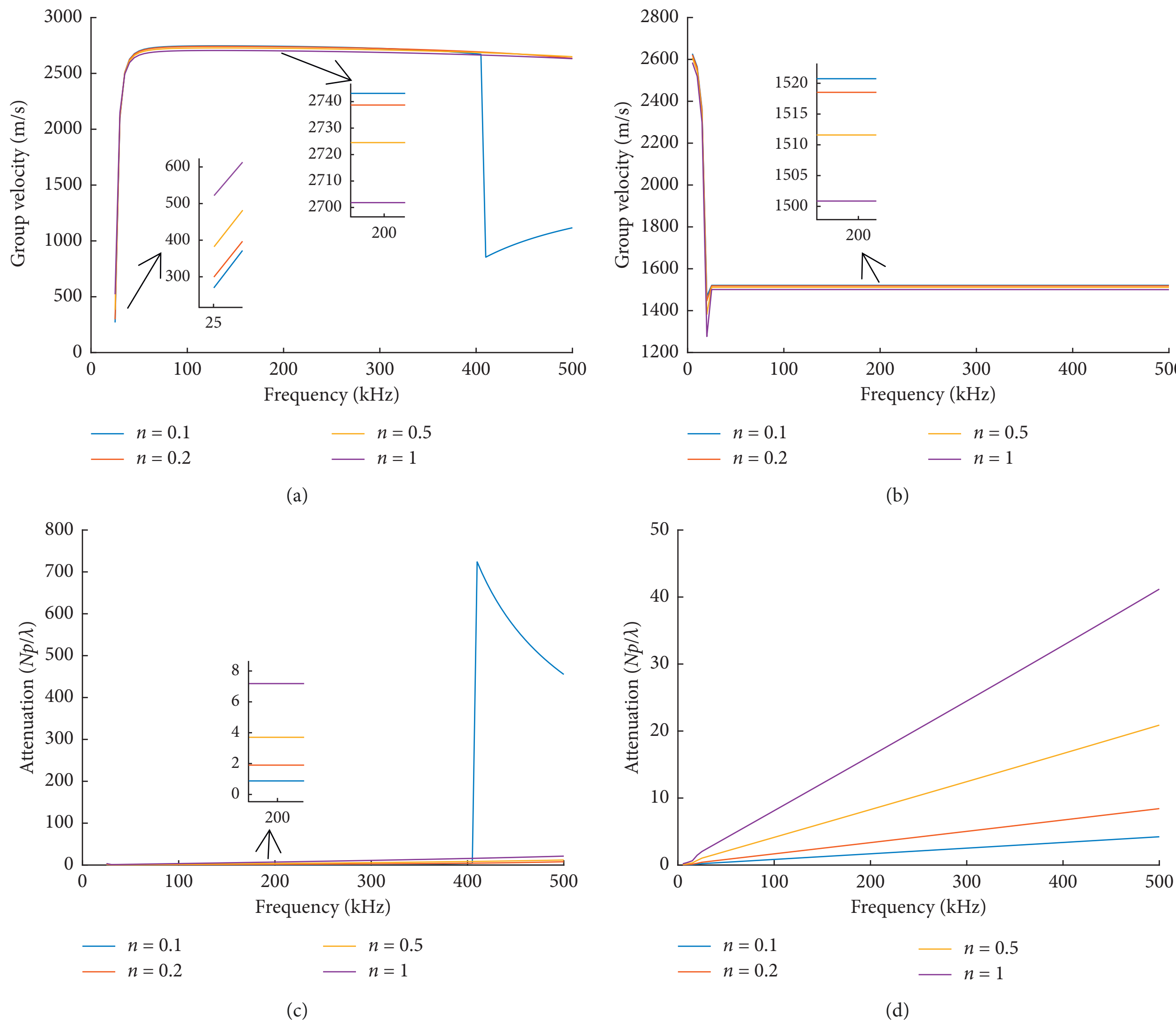

FIGURE 8: Group velocity and attenuation dispersion curves of the guided wave, $n = 0.1$, 0.2, 0.5, and 1. (a) Group velocity curves of $L(0, 2)$. (b) Group velocity curves of $T(0, 1)$. (c) Attenuation curves of $L(0, 2)$. (d) Attenuation curves of $T(0, 1)$.

the plot of attenuation of $L(0, 2)$ and $T(0, 1)$, providing that the attenuation value has a linear relationship with thickness. The maximum attenuation value of $L(0, 2)$ is 130 Np/λ and of $T(0, 1)$ is 158 Np/λ, when $d = 0.4$ mm. Besides, when thickness is 0.4 mm, there is one more $L(0, 3)$ generated in the pipe. When d is 0.05, 0.1, 0.2, and 0.4, A_{L200}, A_{L500}, A_{T200}, and A_{T500} have 6.62, 11.64, 6.15, and 6.66 times growth, respectively.

4.3. Effects of Density of Adhesive Layer on the Dispersion Curve. In the effect study of density on dispersion characteristics, four different density values were set up. As the density decreases, the number of guided modes will increase. Figures 8(a) and 8(b) present the effect of density on group velocity. The results provide that group velocity values are tended to one value, except group velocity of $L(0, 2)$ which decreases sharply from 2617 m/s at 405 kHz to 854 m/s at 410 kHz when $n = 0.1$. When n is 0.1, 0.2, 0.5, and 1, C_{L200}, C_{L500}, C_{T200}, and C_{T500} have 1.50% decrease, 135.42% increase, 1.32% decrease, and 1.38% decrease, respectively (see case 17–case 20). In addition, C_{L500} has a sharp decline, when n is 0.1.

From Figures 8(c) and 8(d), we can see that the attenuation value of $L(0, 2)$ is less than 30 Np/λ and of $T(0, 1)$ is less than 40 Np/λ, except the attenuation of $L(0, 2)$ up to 730 Np/λ at 410 kHz when $n = 0.1$. A_{L200}, A_{L500}, A_{T200}, and A_{T500} have 7.60, 0.95, 8.68, and 8.75 times growth, respectively (see case 17–case 20).

5. Discussion

Figure 9 displays the comparison result of group velocity and attenuation of $L(0, 2)$ and $T(0, 1)$ modes in different adhesive quality. From Figure 9(a), we can see no significant change of group velocity. This result is consistent with the theoretical analysis in the second section: group velocity depends on the real part of the wavenumber; however, body wave attenuation will only affect the imaginary part of the

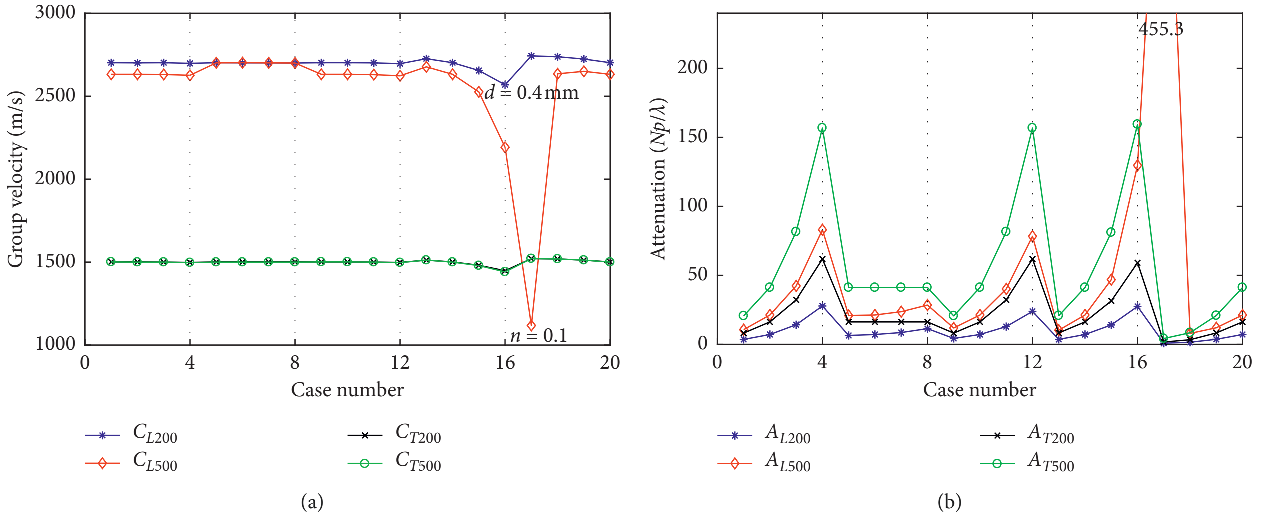

FIGURE 9: Comparison of dispersion characteristics of guided wave. (a) Comparison of group velocity. (b) Comparison of attenuation.

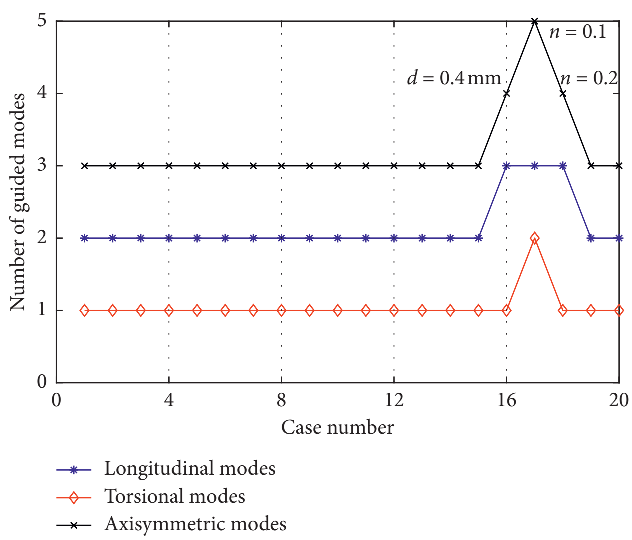

FIGURE 10: Comparison of the guided wave mode numbers.

wavenumber. From the data in Figure 9(b), it is apparent that body wave attenuation of the adhesive layer greatly affects guided wave attenuation. Generally, the guided wave attenuation is mainly determined by the shear wave attenuation, compared with the longitudinal wave. Figure 10 shows the number of guided wave modes propagating in the waveguide under various models. The attenuation of the bonding layer will not affect the number of guided wave modes, but the increase in thickness and density will lead to the increase in the number, which will increase the difficulty of guided wave mode separation and signal processing.

6. Conclusion

The propagation of guided waves in composite structures with a viscoelastic adhesive layer is a difficult topic, which has been rarely reported. In this investigation, the aim was to assess how the viscoelastic parameters, such as attenuation coefficients of body wave, thickness, and density of adhesive affect the dispersion characteristics of the GFRP/adhesive/GFRP pipes. Results show that guided wave attenuation increases with the increase in body wave attenuation of the adhesive layer, but group velocity does not change significantly. Body wave attenuation only affects the imaginary part of the wavenumber, but the group velocity is determined by the real part of the wavenumber; guided waves in higher frequency will have higher attenuation; body wave attenuation does not result in the change of guided wave modes' number; the increase in the thickness and density of the adhesive layer will lead to an increase in guided wave attenuation and modes number. Therefore, the attenuation value of the guided wave mode can reflect the material properties of the adhesive layer and the adhesive quality. The attenuation study of guided waves propagating in composite pipes contributes a theoretical basis to evaluate the bonding quality of the adhesive layer. On the other hand, the significance of analyzing the attenuation dispersion characteristics is to ensure that the attenuation value at the detection frequency is the lowest in practical engineering application, so as to ensure the sensitivity, reliability, and accuracy of detection.

Data Availability

The data used to support the findings of this study are available from the corresponding author upon request.

Conflicts of Interest

There are no conflicts of interest regarding the publication of this article.

Acknowledgments

Thanks are due to Prof. Han and Dr. Qin for their academic supervision and personal support. This work has been supported by the Emergency Management Project of the Natural Science Foundation of China (grant no. 61842103), the Youth Science Foundation (grant no. 11604304), and the Natural Science Foundation of Shanxi, China (grant no. 201801D121156).

References

[1] H. L. Zhang and X. C. Yin, "Guided circumferential waves in double-layered Hollow composite cylinder with welded interface," *Nanjing Li Gong Daxue Xuebao/Journal of Nanjing University of Science & Technology*, vol. 32, no. 4, pp. 482–486, 2008.

[2] M. H. S. Siqueira, C. E. N. Gatts, R. R. da Silva, and J. M. A. Rebello, "The use of ultrasonic guided waves and wavelets analysis in pipe inspection," *Ultrasonics*, vol. 41, no. 10, pp. 785–797, 2004.

[3] A. Demma, M. Lowe, P. Cawley, and B. Pavlakovic, "The effect of bends on the propagation of guided waves in pipes," *Journal of Pressure Vessel Technology*, vol. 127, no. 3, pp. 328–335, 2005.

[4] F. Tian, Y. Jiao, G. Li, G. Sun, and Y. Zhao, "The effect of defect depth on reflection coefficient of ultrasonic guided waves in steel pipes," in *Proceedings of the 2010 International Conference on Wavelet Analysis and Pattern Recognition*, pp. 250–254, Qingdao, China, July 2010.

[5] R. Raišutis, R. Kažys, L. Mažeika et al., "An adjustment-free NDT technique for defect detection in multilayered composite constructions using ultrasonic guided waves," *International Journal of Structural Stability & Dynamics*, vol. 14, no. 8, Article ID 1440025, 2014.

[6] R. Kažys, E. Žukauskas, L. Mažeika, and R. Raišutis, "Propagation of ultrasonic shear horizontal waves in rectangular waveguides," *International Journal of Structural Stability & Dynamics*, vol. 16, no. 8, Article ID 1550041, 2016.

[7] T. Hayashi and M. Murase, "Defect imaging with guided waves in a pipe," *Journal of the Acoustical Society of America*, vol. 117, no. 4, pp. 2134–2140, 2005.

[8] M. V. Predoi, "Guided waves dispersion equations for orthotropic multilayered pipes solved using standard finite elements code," *Ultrasonics*, vol. 54, no. 7, pp. 1825–1831, 2014.

[9] P. B. Nagy and L. Adler, "Nondestructive evaluation of adhesive joints by guided waves," *Journal of Applied Physics*, vol. 66, no. 10, pp. 4658–4663, 1989.

[10] W. Luo, J. L. Rose, J. K. V. Velsor, M. Avioli, and J. Spanner, "Circumferential guided waves for defect detection in coated pipe," in *Review of Progress in Quantitative Nondestructive Evaluation*, vol. 25, pp. 165–172, Springer, Berlin, Germany, 2006.

[11] W. Li and Y. Cho, "Thermal fatigue damage assessment in an isotropic pipe using nonlinear ultrasonic guided waves," *Experimental Mechanics*, vol. 54, no. 8, pp. 1309–1318, 2014.

[12] M. Vasiljevic, T. Kundu, W. Grill, and E. Twerdowski, "Recent advances on pipe inspection using guided waves generated by electromagnetic acoustic transducers," in *Proceedings of the Health Monitoring of Structural and Biological Systems 2008*, vol. 6935, San Diego, CA, USA, March 2008.

[13] F. Song, G. L. Huang, and K. Hudson, "Guided wave propagation in honeycomb sandwich structures using a piezoelectric actuator/sensor system," *Smart Materials and Structures*, vol. 18, no. 12, Article ID 125007, 2009.

[14] J. M. Lees, "Behaviour of GFRP adhesive pipe joints subjected to pressure and axial loadings," *Composites Part A: Applied Science and Manufacturing*, vol. 37, no. 8, pp. 1171–1179, 2006.

[15] W. Ge, J. Deng, F. Chen, H. Cheng, and Y. Ling, "Exploitation and application of bamboo fiber-reinforced filament-wound pressure pipe," *Scientia Silvae Sinicae*, vol. 52, no. 4, pp. 127–131, 2016.

[16] H. M. Matt, "Structural diagnostics of CFRP composite aircraft components by ultrasonic guided waves and built-in piezoelectric transducers," Thesis/Dissertation, University of California, vol. 126, no. 7, p. 14, San Diego, CA, USA, 2007.

[17] P. J. Shorter, "Wave propagation and damping in linear viscoelastic laminates," *The Journal of the Acoustical Society of America*, vol. 115, no. 5, pp. 1917–1925, 2004.

[18] A. Lhémery, V. Baronian, and B. Chapuis, "Guided wave propagation and scattering in pipeworks comprising elbows: theoretical and experimental results," in *Proceedings of the 13th Anglo-French Physical Acoustics Conference*, London, UK, January 2014.

[19] F. Yan, "Ultrasonic guided wave phased array for isotropic and anisotropic plates," Dissertations & Theses-radworks, Proquest, Ann Arbor, MI, USA, 2008.

[20] F. L. D. Scalea, P. Rizzo, and A. Marzani, "Propagation of ultrasonic guided waves in lap-shear adhesive joints," *The Journal of the Acoustical Society of America*, vol. 115, no. 1, pp. 146–156, 2004.

[21] Z. Hong, "Analysis of guided waves in adhesively bonded composite structures," *Journal of Applied Sciences*, vol. 13, no. 22, pp. 5298–5308, 2013.

[22] E. Siryabe, M. Renier, A. Meziane, and M. Castaings, "The transmission of lamb waves across adhesively bonded lap joints to evaluate interfacial adhesive properties," *Physics Procedia*, vol. 70, pp. 541–544, 2015.

[23] M. Castaings, "SH ultrasonic guided waves for the evaluation of interfacial adhesion," *Ultrasonics*, vol. 54, no. 7, pp. 1760–1775, 2014.

[24] M. Kharrat, M. N. Ichchou, O. Bareille, and W. Zhou, "Pipeline inspection using a torsional guided-waves inspection system. Part 1: defect identification," *International Journal of Applied Mechanics*, vol. 6, no. 4, Article ID 1450034, 2014.

[25] E. Rojas, A. Baltazar, and K. J. Loh, "Damage detection using the signal entropy of an ultrasonic sensor network," *Smart Materials & Structures*, vol. 24, no. 7, Article ID 075008, 2015.

[26] J. L. Rose, *Ultrasonic Guided Waves in Solid Media*, Cambridge University Press, Cambridge, UK, 2014.

[27] V. Agostini, P. P. Delsanto, I. Genesio, and D. Olivero, "Simulation of lamb wave propagation for the characterization of complex structures," *IEEE Transactions on Ultrasonics Ferroelectrics & Frequency Control*, vol. 50, no. 4, pp. 441–448, 2003.